Supporting Information for

Unusual isosymmetric order-disorder phase transition in the new perovskite-type dimethylhydrazinium manganese formate exhibiting weak ferromagnetism and photoluminescent properties

by J.A. Zienkiewicz, D. Kowalska, K. Fedoruk, M. Stefański, A. Pikul, M. Ptak

Content:

Fig. S1. The asymmetric unit at 300 K (HT phase) (a) and at 100 K (LT phase) (b) showing the atom numbering scheme. Displacement ellipsoids are drawn at the 50 % probability level. In the HT phase the DMHy$^+$ cation is disordered over three positions with the same ratio ⅓ (the positions disordered over C and N atoms are presented as octants). [Symmetry codes: ^{i} −x, −y+1, −z+2; ^{ii} −x+1, −y+2, −z+2.]
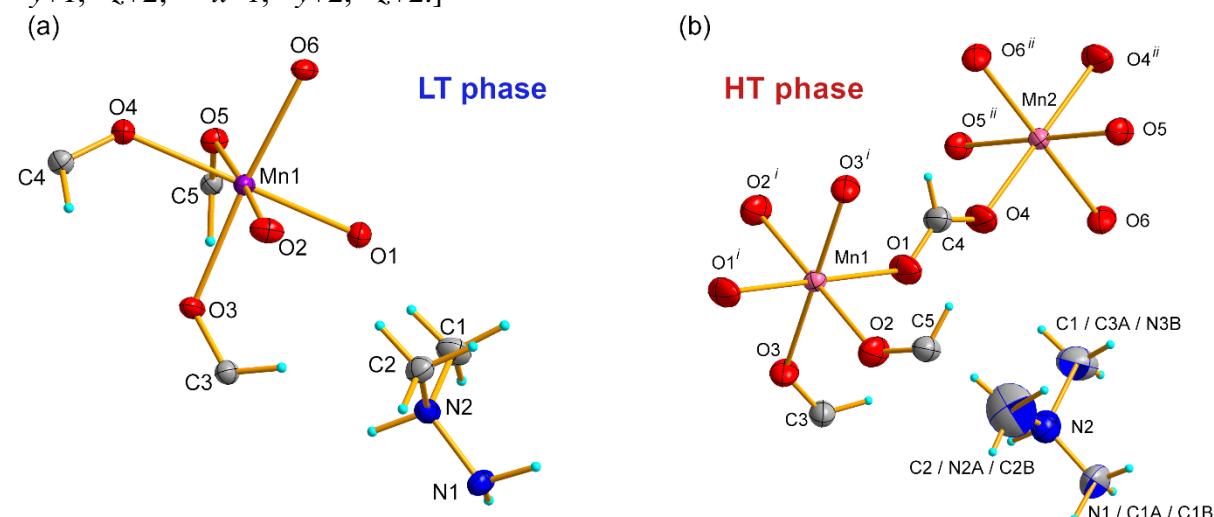
Fig. S2. Powder XRD pattern for the as-prepared bulk sample of [DMHy]Mn(HCOO)$_3$ together with the simulated one based on the single crystal structure refined at 300 K
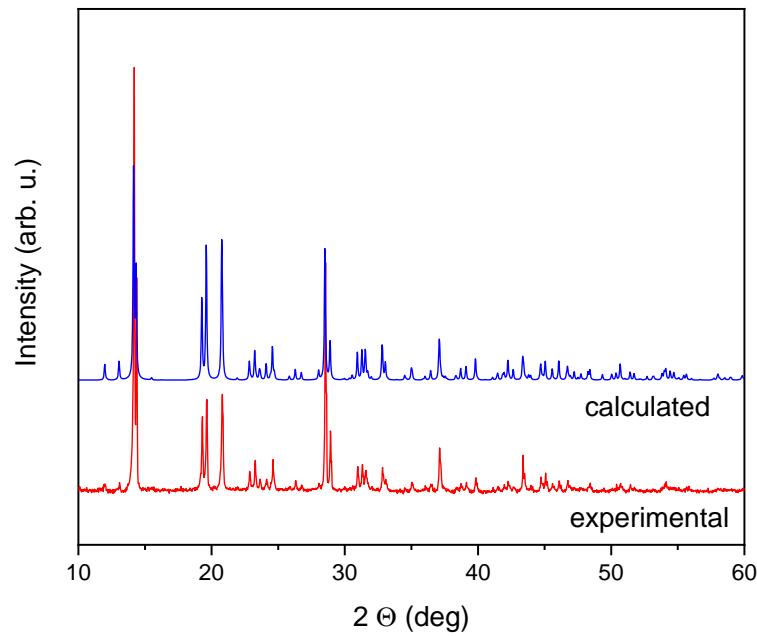
Fig. S3. The DSC traces measured in a cooling and heating runs
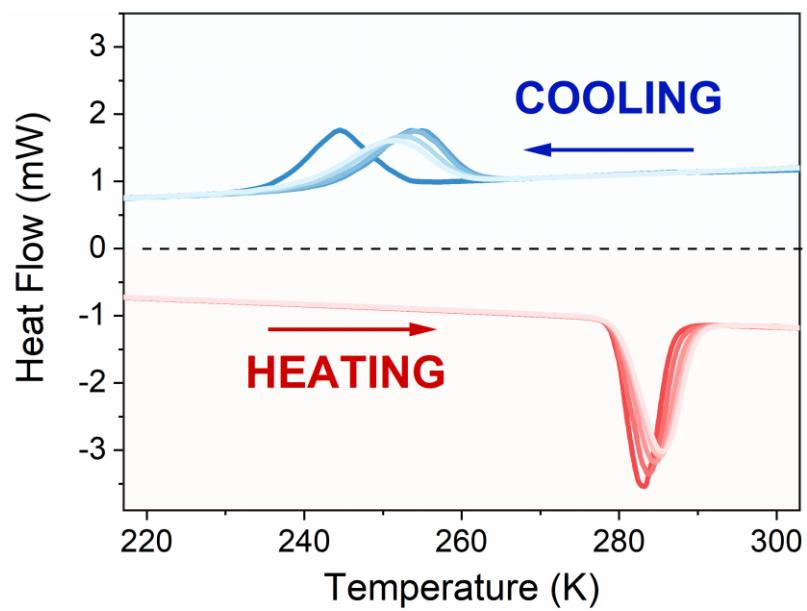
Fig. S4. The temperature dependence of the dielectric loss ε'' of [DMHy]Mn(HCOO)$_3$ measured for (a) single crystal in the [110] directions, (b) single crystal in the perpendicular to [110] direction, (c) a pellet. The representative curves are plotted in frequency decades between 10^3 Hz and 10^6 Hz. The vertical lines correspond to the phase-transition temperatures obtained from the dynamic DSC measurements
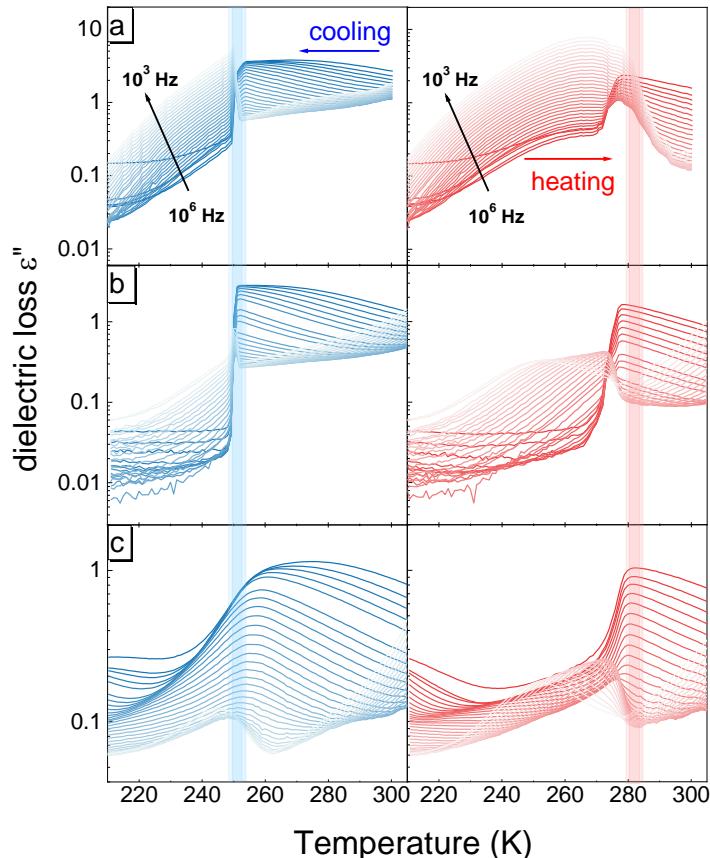
Fig. S5. Relaxation times as a function of 1000/T. The blue points correspond to the curves obtained during cooling, and the red points during heating. The inset shows the frequency-dependent dielectric loss measured at 250 K (on cooling) and 275 K (on heating).
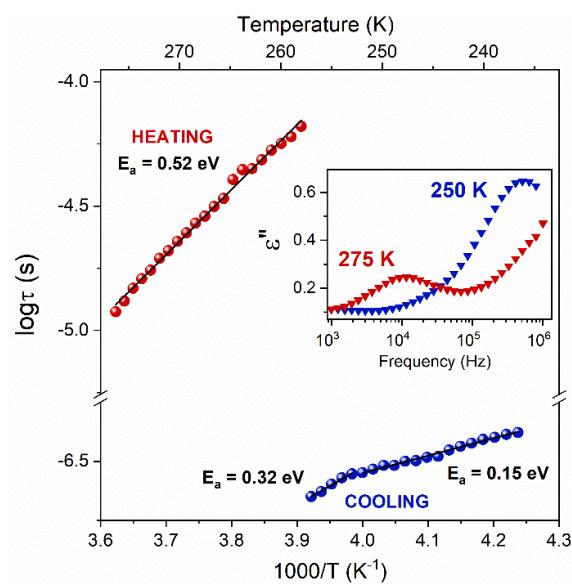
Fig. S6. The result of determining the energy band gap (E_g) using the Kubelka-Munk theory for the [DMHy]Mn(HCOO)$_3$ crystals
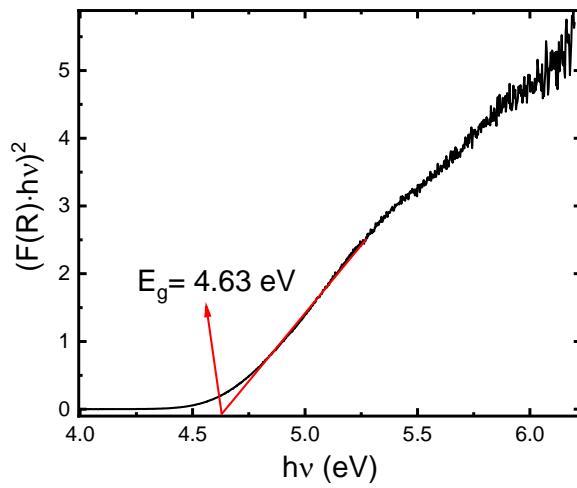
Fig. S7. Activation energy of the thermal quenching of emission bands of [DMHy]Mn(HCOO)$_3$ crystals excited at 266 nm
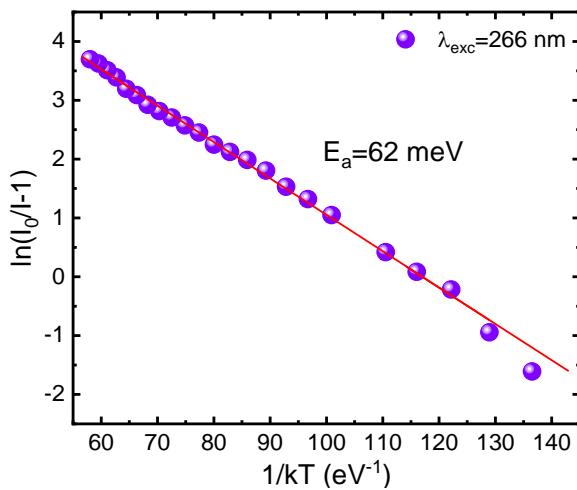
Fig. S8. The luminescence decay profile of [DMHy]Mn(HCOO)$_3$ crystals excited at 266 nm and monitored at 725 nm recorded at 77 K
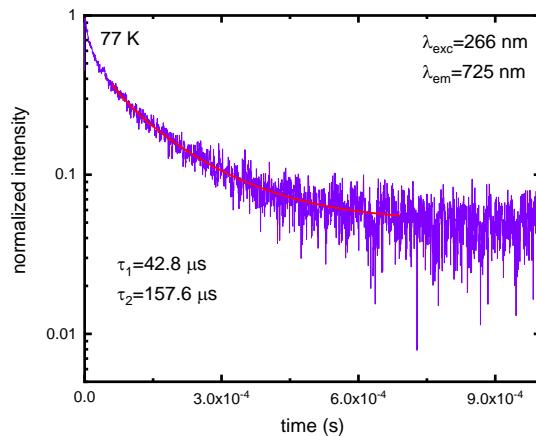
Tab. S1. Hydrogen-bond geometry for [DMHy]Mn(HCOO)$_3$

| D—H$\cdots A$	D—H (Å)	H$\cdots A$ (Å)	$D \cdots A$ (Å)	D—H$\cdots A$ (°)
HT phase (300 K)				
N1—H1$A \cdots$O2^i	1.03	2.58	3.537 (10)	154
N1—H1$B \cdots$O6^{ii}	1.03	2.16	3.040 (6)	143
N2—H2$\cdots$O5^{iii}	0.98	1.84	2.811 (3)	173
C1—H1D$\cdots$O3^{iv}	0.96	2.57	3.432 (10)	149
C1—H1$E \cdots$O4	0.96	2.37	3.265 (10)	154
N1A—H1$AB \cdots$O1^v	1.03	2.55	3.412 (8)	140
N1A—H1$AB \cdots$O2^{vi}	1.03	2.44	3.207 (6)	131
C1A—H1$AC \cdots$O3^{iv}	0.96	2.45	3.359 (7)	157
C1A—H1$AD \cdots$O4	0.96	2.51	3.428 (8)	161
C2A—H2$AC \cdots$O1	0.96	2.38	3.305 (12)	163
LT phase (100 K)				
N1—H1A$\cdots$O6^{ii}	1.00	1.99	2.961 (3)	163
N1—H1B$\cdots$O1^{vii}	0.99	2.09	3.072 (3)	177
N1—H1B$\cdots$O4^v	0.99	2.53	3.172 (4)	123
N2—H2$\cdots$O4^v	0.98	2.60	3.133 (3)	115
N2—H2$\cdots$O5^v	0.98	1.94	2.846 (3)	152
C2—H2A$\cdots$O2^{viii}	0.96	2.52	3.267 (4)	135
C2—H2B$\cdots$O5^{ix}	0.96	2.37	3.321 (4)	169
C2—H2C$\cdots$O3^{iv}	0.96	2.55	3.456 (4)	157

Symmetry codes: ^{i} $-x+1/2$, $y+1/2$, $-z+3/2$; ^{ii} $-x+3/2$, $y-1/2$, $-z+3/2$; ^{iii} $x-1/2$, $-y+3/2$, $z-1/2$; ^{iv} $x+1$, y, z; ^{v} $-x+1/2$, $y-1/2$, $-z+3/2$; ^{vi} $x+1/2$, $-y+1/2$, $z-1/2$; ^{vii} $-x+1$, $-y+1$, $-z+1$; ^{viii} $-x+1$, $-y+1$, $-z+2$; ^{ix} $x+1/2$, $-y+3/2$, $z+1/2$.

All e.s.d.'s (except the e.s.d. in the dihedral angle between two l.s. planes) are estimated using the full covariance matrix. The cell e.s.d.'s are taken into account individually in the estimation of e.s.d.'s in distances, angles and torsion angles; correlations between e.s.d.'s in cell parameters are only used when they are defined by crystal symmetry. An approximate (isotropic) treatment of cell e.s.d.'s is used for estimating e.s.d.'s involving l.s. planes.

Tab. S2. Selected geometric parameters (Å, °) in [DMHy]Mn(HCOO)$_3$

HT phase (300 K)			
Mn1—O1	2.1773 (16)	O1—C4	1.225 (3)
Mn1—O1^i	2.1773 (16)	O2—C5	1.224 (3)
Mn1—O2	2.1864 (16)	O3—C3	1.233 (3)
Mn1—O2^i	2.1864 (16)	O4—C4	1.229 (3)
Mn1—O3	2.1875 (17)	O5—C5^{iii}	1.256 (3)
Mn1—O3^i	2.1875 (17)	O6—C3^{iv}	1.229 (3)

Mn2—O4	2.1681 (16)	N1—N2	1.482 (6)
Mn2—O4^{ii}	2.1681 (16)	N2—C1	1.398 (10)
Mn2—O5	2.2046 (15)	N2—C2	1.476 (10)
Mn2—O5^{ii}	2.2046 (15)	N2—N1A	1.428 (6)
Mn2—O6	2.1873 (16)	N2—C1A	1.538 (8)
Mn2—O6^{ii}	2.1873 (16)	N2—C2A	1.538 (8)

LT phase (100 K)

Mn1—O4	2.173 (2)	O3—C3	1.251 (3)
Mn1—O5	2.199 (2)	O6—C3^{iv}	1.256 (3)
Mn1—O3	2.190 (2)	N1—N2	1.447 (3)
Mn1—O6	2.180 (2)	O2—C5^{vi}	1.252 (4)
Mn1—O2	2.188 (2)	O1—C4^{vii}	1.248 (4)
Mn1—O1	2.181 (2)	N2—C2	1.488 (4)
O4—C4	1.246 (4)	N2—C1	1.490 (4)
O5—C5	1.267 (4)		

HT phase (300 K)

O1—Mn1—O1^{i}	180.0	O6—Mn2—O5	87.93 (6)
O1^{i}—Mn1—O2^{i}	89.44 (7)	O6—Mn2—O5^{ii}	92.07 (6)
O1^{i}—Mn1—O2	90.56 (7)	O6^{ii}—Mn2—O6	180.0
O1—Mn1—O2^{i}	90.56 (7)	C4—O1—Mn1	133.92 (15)
O1—Mn1—O2	89.44 (7)	C5—O2—Mn1	136.81 (15)
O1^{i}—Mn1—O3	90.64 (7)	C3—O3—Mn1	127.76 (16)
O1^{i}—Mn1—O3^{i}	89.36 (7)	C4—O4—Mn2	134.89 (16)
O1—Mn1—O3^{i}	90.64 (7)	C5^{iii}—O5—Mn2	126.38 (14)
O1—Mn1—O3	89.36 (7)	C3^{iv}—O6—Mn2	132.23 (16)
O2^{i}—Mn1—O2	180.0	O6^{v}—C3—O3	128.4 (2)
O2^{i}—Mn1—O3	93.37 (6)	O1—C4—O4	127.6 (2)
O2—Mn1—O3^{i}	93.37 (6)	O2—C5—O5^{iii}	125.5 (2)
O2^{i}—Mn1—O3^{i}	86.63 (6)	N1—N2—C1A	102.7 (4)
O2—Mn1—O3	86.63 (6)	C1—N2—N1	113.7 (5)
O3—Mn1—O3^{i}	180.0	C1—N2—C2	109.2 (6)
O4—Mn2—O4^{ii}	180.0	C1—N2—N1A	120.6 (5)
O4—Mn2—O5^{ii}	85.91 (7)	C1—N2—C1A	12.5 (5)
O4^{ii}—Mn2—O5	85.91 (7)	C1—N2—C2A	98.0 (6)
O4—Mn2—O5	94.09 (7)	C2—N2—N1	113.4 (5)
O4^{ii}—Mn2—O5^{ii}	94.09 (7)	C2—N2—C1A	120.6 (5)
O4—Mn2—O6^{ii}	91.06 (6)	C2—N2—C2A	15.3 (6)
O4^{ii}—Mn2—O6	91.06 (6)	N1A—N2—N1	19.2 (3)
O4—Mn2—O6	88.94 (6)	N1A—N2—C2	94.5 (5)

O4^{ii}—Mn2—O6^{ii}	88.94 (6)	N1A—N2—C1A	112.1 (4)
O5—Mn2—O5^{ii}	180.00 (9)	N1A—N2—C2A	109.5 (5)
O6^{ii}—Mn2—O5^{ii}	87.93 (6)	C2A—N2—N1	128.5 (5)
O6^{ii}—Mn2—O5	92.07 (6)	C2A—N2—C1A	110.2 (5)

LT phase (100 K)

O4—Mn1—O5	81.16 (8)	O1—Mn1—O2	94.70 (10)
O4—Mn1—O3	92.50 (8)	C4—O4—Mn1	130.7 (2)
O4—Mn1—O6	90.94 (8)	C5—O5—Mn1	126.5 (2)
O4—Mn1—O2	96.20 (9)	C3—O3—Mn1	121.37 (16)
O4—Mn1—O1	168.79 (9)	C3^{iv}—O6—Mn1	129.81 (17)
O3—Mn1—O5	92.58 (8)	C5^{vi}—O2—Mn1	132.2 (2)
O6—Mn1—O5	94.38 (8)	O2^{viii}—C5—O5	125.0 (3)
O6—Mn1—O3	172.64 (7)	C4^{ix}—O1—Mn1	134.1 (2)
O6—Mn1—O2	87.41 (8)	O4—C4—O1^{x}	124.4 (3)
O6—Mn1—O1	92.14 (8)	N1—N2—C2	109.0 (2)
O2—Mn1—O5	176.82 (8)	N1—N2—C1	114.2 (2)
O2—Mn1—O3	85.75 (8)	C2—N2—C1	111.2 (2)
O1—Mn1—O5	87.86 (9)	O3—C3—O6^{v}	125.1 (2)
O1—Mn1—O3	85.72 (8)		
Br3—Pb1—Br1	92.973 (8)		

Symmetry codes: ^{i} −x, −y+1, −z+2; ^{ii} −x+1, −y+2, −z+2; ^{iii} −x+1, −y+1, −z+2; ^{iv} −x+1/2, y+1/2, −z+3/2; ^{v} −x+1/2, y−1/2, −z+3/2; ^{vi} x+1/2, −y+3/2, z+1/2; ^{vii} x+1/2, −y+3/2, z−1/2; ^{viii} x−1/2, −y+3/2, z−1/2; ^{ix} x−1, y, z; ^{x} x−1/2, −y+3/2, z+1/2.

Tab. S3. The temperature-dependent isosymmetric PTs reported for single and double 3D hybrid perovskites

Compound	LT → HT	T (K) [a]	Order	TF	Ref.
Perovskites					
[DMHy]Mn(HCOO)$_3$	$P2_1/n \to P2_1/n$	250.9 / 281.9	1st	1.01	[b]
[Im]Mg(HCOO)$_3$	$P2_1/n \to P2_1/n$	451 / 448	2nd	0.90	[1,2]
[MA]Mn(N$_3$)$_3$ [c]	$P2_1/c \to P2_1/c$	280 / 263	1st	0.84	[3,4]
[GA]SnCl$_3$	$Pnma \to Pnma$	419 / 409	1st	1.18 5	[5,6]
Double perovskite					
[DMA]$_2$KCo(CN)$_6$	$P4/mnc \to P4/mnc$	249 / 241	1st	0.96	[7]
[DMA]$_2$KCr(CN)$_6$	$P4/mnc \to P4/mnc$	218 / 215	1st	0.95	[8]
[DMA]$_2$KFe(CN)$_6$	$P4/mnc \to P4/mnc$	228 / 227	1st	0.96	[9,10]
[Im]$_2$KCo(CN)$_6$	$R\bar{3}m \to R\bar{3}m$	198	[d]	0.93	[11]
[Im]$_2$KFe(CN)$_6$	$R\bar{3}m \to R\bar{3}m$	187	2nd	0.93	[12]
[Tz]$_2$KCo(CN)$_6$	$Cmcm \to Cmcm$	237	1st	1.07	[13]

Key: [a] on heating/cooling, if given; [b] this work; [c] both (LT and HT) phases are ordered; [d] not given; [e] not calculated; Im$^+$, imidazolium; MA$^+$, methylammonium; GA$^+$, guanidinium, DMA$^+$, dimethylammonium; Tz$^+$, thiazolium

1   M. Mączka, N. L. Marinho Costa, A. Gągor, W. Paraguassu, A. Sieradzki and J. Hanuza, *Phys. Chem.*

Chem. Phys., 2016, **18**, 13993–14000.

2   G. Kieslich, S. Sun and A. K. Cheetham, *Chem. Sci.*, 2014, **5**, 4712–4715.

3   X. H. Zhao, X. C. Huang, S. L. Zhang, D. Shao, H. Y. Wei and X. Y. Wang, *J. Am. Chem. Soc.*, 2013, **135**, 16006–16009.

4   G. Kieslich, S. Sun and A. K. Cheetham, *Chem. Sci.*, 2015, **6**, 3430–3433.

5   M. Szafrański and K. Ståhl, *J. Solid State Chem.*, 2007, **180**, 2209–2215.

6   T. Oku, *Rev. Adv. Mater. Sci.*, 2020, **59**, 264–305.

7   W. Zhang, H.-Y. Ye, R. Graf, H. W. Spiess, Y.-F. Yao, R.-Q. Zhu and R.-G. Xiong, *J. Am. Chem. Soc.*, 2013, **135**, 5230–5233.

8   M. Rok, G. Bator, B. Zarychta, B. Dziuk, J. Repeć, W. Medycki, M. Zamponi, G. Usevičius, M. Šimenas and J. Banys, *Dalt. Trans.*, 2019, **48**, 4190–4202.

9   M. Rok, G. Bator, W. Medycki, M. Zamponi, S. Balčiūnas, M. Šimėnas and J. Banys, *Dalt. Trans.*, 2018, **47**, 17329–17341.

10   W.-J. Xu, S.-L. Chen, Z.-T. Hu, R.-B. Lin, Y.-J. Su, W.-X. Zhang and X.-M. Chen, *Dalt. Trans.*, 2016, **45**, 4224–4229.

11   X. Zhang, X. D. Shao, S. C. Li, Y. Cai, Y. F. Yao, R. G. Xiong and W. Zhang, *Chem. Commun.*, 2015, **51**, 4568–4571.

12   W. Zhang, Y. Cai, R.-G. Xiong, H. Yoshikawa and K. Awaga, *Angew. Chemie Int. Ed.*, 2010, **49**, 6608–6610.

13   Z. X. Gong, Q. W. Wang, J. J. Ma, J. Y. Jiang, D. Y. E, Z. Q. Li, F. W. Qi and H. Liang, *Mater. Chem. Front.*, 2020, **4**, 918–923.